JOURNAL OF MATERIALS SCIENCE **39** (2004) 7351 – 7357

On glass formation for a $Na_2O{\cdot}4TeO_2$ melt: Effect of melting temperature, time, and raw material

DONGMEI ZHU
Ceramic Engineering Department and Graduate Center for Materials Research, University of Missouri-Rolla, Rolla, MO 65409, USA; State Key Laboratory of Solidification Processing, Northwestern Polytechnic University, Xi'an, Shaanxi 710072, People's Republic of China
E-mail: dzhu@umr.edu

C. S. RAY
Ceramic Engineering Department and Graduate Center for Materials Research, University of Missouri-Rolla, Rolla, MO 65409, USA

WANCHENG ZHOU
State Key Laboratory of Solidification Processing, Northwestern Polytechnic University, Xi'an, Shaanxi 710072, People's Republic of China

D. E. DAY
Ceramic Engineering Department and Graduate Center for Materials Research, University of Missouri-Rolla, Rolla, MO 65409, USA

The effect of melting temperature, time, and the type of raw material, $NaNO_3$ or Na_2CO_3, as a source for Na_2O on the glass formation for a $Na_2O{\cdot}4TeO_2(NT_4)$ melt was investigated. Melting with $NaNO_3$ at 750°C for a short time (15 min) produced a glass that is slightly more chemically durable and more resistant to crystallization than glasses melted at a higher temperature (800°C), or for a longer time (60 min), or using Na_2CO_3. A thin surface layer ($<$1.5 nm) that contains some nitrogen and a higher concentration of bridging oxygen is suspected to be the reason for the higher chemical durability and higher resistance to crystallization for this glass. However, melting at 800°C for 60 min produced a glass, whose properties were independent of the type of raw material, $NaNO_3$ or Na_2CO_3, used.

1. Introduction

Tellurite glasses are of interest because of their low melting temperatures (530 to 830°C) and promising optical and electrical properties, such as a high refractive index (generally >2), and, hence, a high dielectric constant, IR transmission up to 6 μm and a large third order non-linear optical susceptibility. These unique optical and electrical properties make tellurite glasses potential candidate materials for IR window, all-optical switching devices and laser hosts [1–5].

Pure tellurium oxide (TeO_2) does not easily form a glass by conventional melting methods. The structure of crystalline TeO_2 consists of TeO_4 trigonal bipyramid (tbp) with a lone pair of electrons at one of the equatorial positions. On cooling a TeO_2 melt, the presence of the lone pair of electrons greatly restricts the structural rearrangement of the TeO_4 groups, that is favorable for glass formation. A pure TeO_2 glass can be prepared only in milligram quantities using very high cooling rates, such as roller-quenching [6] or vapour deposition [7]. Further more, a pure TeO_2 glass has a poor chemically durability and crystallizes easily.

Adding small amounts of modifier oxides, such as alkali or alkaline-earth, dramatically improves the glass formation tendency of the TeO_2 melt [7–10]. In previous studies [7, 8], large quantities (~50 g) of stable and chemically durable Na_2O-TeO_2 glasses were routinely prepared without problems. The glass forming tendency of these sodium tellurite melts was found to be composition dependent, being highest for the $20Na_2O$-$80TeO_2$, mol% (NT_4) glass. The Raman spectra showed [11–13] that the structure of sodium-tellurite glasses containing $\leq$20 mol% Na_2O consists of corner-sharing continuous random network of TeO_4 tbp's and TeO_{3+1} polyhedra having one non-bridging oxygen (NBO). For the glasses $\geq$20 mol% Na_2O, TeO_3 trigonal pyramids continue to form primarily at the expense of TeO_4 tbp's, thereby, forming more NBO's in the structure and reducing the stability of the glasses.

In previous studies [7, 8], we noted some interesting events while melting sodium tellurite glasses. An evaporation from the melt occurred during melting(750–800°C) and the properties, at least the thermal properties, were found to depend on the type of raw materials used as a source for Na_2O, namely, Na_2CO_3 or $NaNO_3$. Crystalline α-TeO_2 powder was used as a source for TeO_2. The material condensed from the species evaporating from the melt was later identified as amorphous particles of pure TeO_2, free of Na_2O. This seems reasonable since the vapour pressure of TeO_2 is larger than that of Na_2O, for example, at 727°C the vapour pressure of TeO_2 is about 1.3×10^{-1} mm Hg compared to a vapour pressure of 1.5×10^{-3} mm Hg for Na_2O [14]. This higher vapour pressure of TeO_2 causes TeO_2, not Na_2O, to evaporate from the sodium tellurite melts.

Any evaporation of TeO_2 during melting will change the composition of the glass from its target composition, i.e., it lowers the TeO_2 content of the glass. This compositional difference between the glass and batch should increase with increasing temperature or time for melting. In the present paper, systematic investigations to determine the compositional change that can occur for a sodium tellurite glass when melted at different temperatures for different times are described. The effect of this compositional change on a few selected thermal properties, such as the glass transition and crystallization temperatures, that are relevant to assessing the glass formation tendency of a melt or the stability of a glass, was investigated. The NT_4 composition was chosen as a model. The effect of raw materials, namely, Na_2CO_3 or $NaNO_3$ on the above thermal properties of the NT_4 glass was also investigated. The temperature and time that are most suitable for melting sodium tellurite glasses were determined, and the advantages and disadvantages of using Na_2CO_3 or $NaNO_3$ for the source of Na_2O were explored.

2. Experimental

Batches that produced 20 g of the $20Na_2O–80TeO_2$, mol%, (NT_4) glass were prepared by dry-mixing crystalline powders of α-TeO_2 (99.95% purity) and Na_2CO_3 (99.95%) or $NaNO_3$ (99.99%) in appropriate proportions. These mixtures (batches) were then melted at 750°C for 15 min, 750°C for 60 min, 800°C for 20 min, or 800°C for 60 min in platinum crucible in air. The melt was quenched between two steel plates to produce a glass plate of about 2 mm thickness, which was stored in a vacuum desiccator.

The amorphous character of the glasses was confirmed by X-ray diffraction analysis (XRD). No platinum was detectable in any of these glasses by X-ray fluorescence spectroscopy (XRF), which suggests that the dissolution of platinum from the crucible into the melt was negligible. The average composition as measured by energy dispersive X-ray analysis (EDS) for all the glasses was nearly the same, irrespective of the melting temperature, melting time, and raw materials, as the batch composition within an experimental error of ±1.5 wt% for each of the two components, Na_2O and TeO_2.

The glass transition (T_g) and crystallization (T_x) temperatures for the glasses were measured using differential scanning calorimetry (TA-DSC2010) in a flowing nitrogen gas (30 cm^3/min) and a heating rate of 10°C/min. The weight and particle size of the glass sample for each DSC measurement was about 20 mg and 75–160 μm, respectively. The sample was placed in an aluminum pan (TA 900786.901) with a lid (TA 900779.901) on top of the sample and sealed using a crimping die for all the DSC measurements.

The as-quenched glasses were heated at their crystallization temperatures, as measured by DSC, for about 10 h and analyzed by XRD at a scan rate of 2°/min using a XDS2000™ (Scintag Inc.) to identify the crystalline phases.

The Fourier Transform Infrared (FTIR) spectrum (1760-x infrared fourier tranform spectrometer, Perkin Elmer) for each glass was measured from 4000 to 400 cm^{-1} using the standard KBr technique. The IR spectrum for pure KBr was measured first to make the necessary background correction.

To estimate how much the composition of the glass might change due to evaporation of TeO_2 from the melt, the weight-loss was measured for TeO_2 powders melted at 750C or 800°C for 1 to 3 h. Prior to melting, the TeO_2 powders were dried at 120°C for 14 h. The rate of weight loss was calculated from the initial (∼15.41 g) and final (after melting) weight of the sample.

3. Results and discussion

3.1. Evaporation of TeO_2

The cumulative weight loss due to evaporation from the TeO_2 melt at 750 or 800°C is given in Table I as a function of melting time (the melting temperature of TeO_2 is ∼732°C). The rate of weight loss is nearly constant at 0.059% per hour at 750°C, but nearly doubles to 0.131% when the temperature is increased to 800°C. Calculations show that melting this NT_4 glass at 800°C for 1 h may change the composition from its target value of $20Na_2O–80TeO_2$, mol%, ($8.85Na_2O–91.15TeO_2$, wt%) to $20.01Na_2O–79.99TeO_2$, mol%, ($8.86Na_2O–91.14TeO_2$, wt%). This very small change in composition is insignificant to this study. Melting these glasses at temperatures lower than 800°C means the change in composition due to TeO_2 evaporation will even be lower. These results are consistent with the EDS results, where no detectable difference in composition was observed for the sodium tellurite glasses melted at 750 or 800°C for up to 60 min.

3.2. Differential thermal analysis (DSC)

A typical DSC curve at 10°C /min for the NT_4 glass melted at 800°C for 60 min and using Na_2CO_3 as the source for Na_2O is shown in Fig. 1. Fig. 2a and b show the DSC curves for the NT_4 glasses prepared using Na_2CO_3 and $NaNO_3$, respectively, as a function of melting temperature and time. The general features of

TABLE I Weight loss due to evaporation of TeO_2 melted at 750 or 800°C for 1 to 3 h

Temperature (°C)	Time (h)	Cumulative weight loss (g)	Rate of weight loss (% per h)	Average rate of weight loss (% per h)
750	1	0.0086	0.059	0.059
750	2	0.0178	0.058	
750	3	0.0294	0.064	
800	1	0.0213	0.138	0.131
800	2	0.0392	0.127	
800	3	0.0597	0.129	

Initial weight of TeO_2: 15.41 g.

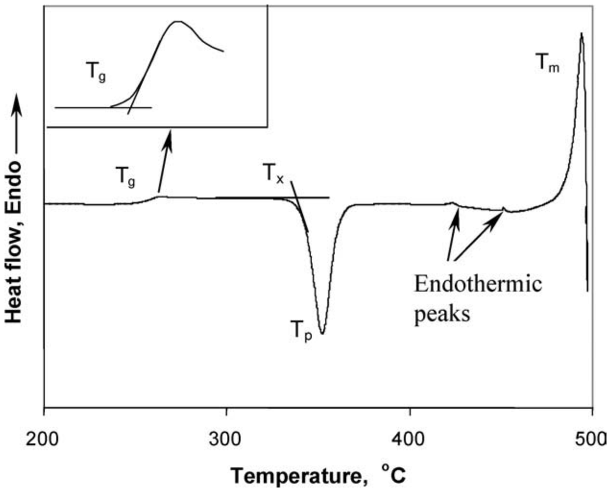

Figure 1 Typical DSC curve at 10°C/min for the NT_4 glass melted at 800°C for 60 min using Na_2CO_3 as the source for Na_2O.

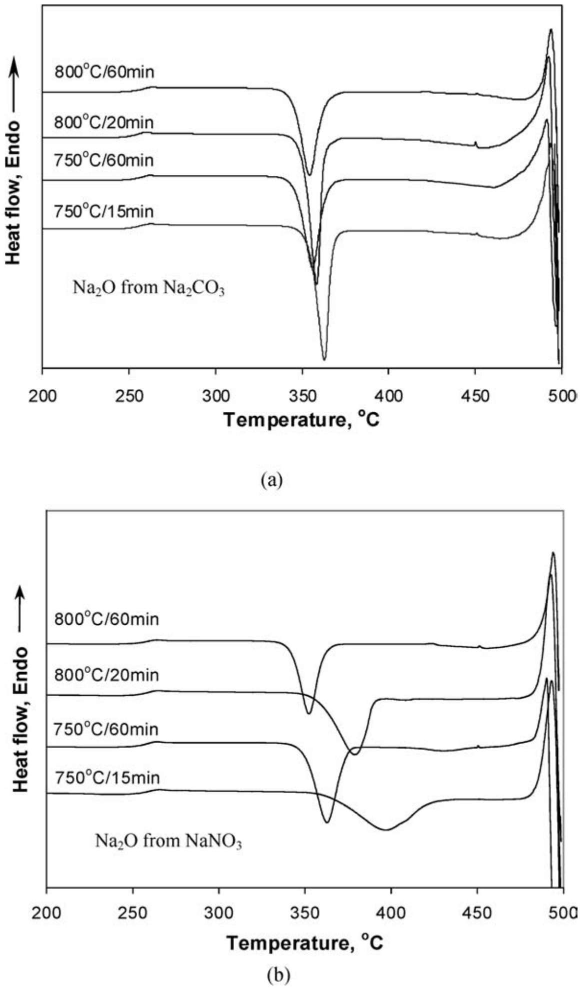

(a)

(b)

Figure 2 DSC curves for the NT_4 glasses melted using either: (a) Na_2CO_3 or (b) $NaNO_3$ for the temperature and time listed on each curve. The curves are displaced intentionally in the vertical direction for clarity.

all these DSC curves are nearly the same, and contain, in increasing temperature, a small endothermic peak (∼255°C), a large exothermic peak (350–370°C), and a large endothermic peak (∼476°C), corresponding to the following transformations; glass transition, crystallization, and melting, respectively. The glass transition temperature, T_g, onset temperature for crystallization, T_x, crystallization peak temperature, T_p, and the melting temperature T_m, as determined from these DSC curves are given in Table II.

It is to be noted that the DSC curves for these glasses, particularly those melted at 800°C or for a longer time, contain two additional small endothermic peaks at about 425 and 450°C as shown by arrows in Fig. 1. Although, these peaks are barely detectable, their consistent appearance caught our attention. The reason for these two small peaks is not understood at this time, but may be an experimental artifact, a reaction of the glass with the alumina pan, or some small transformation in the crystallized sample. Further investigation to understand the reason for these peaks in the sodium tellurite glasses is in progress.

Irrespective of the melting temperature, time, or raw material, the T_g or T_m for all these glasses is nearly the same ($T_g \sim 255 \pm 1$°C, $T_m \sim 476 \pm 1$°C), see Fig. 2 and Table II. The 476°C melting temperature is very close to the 470°C melting temperature reported [15] for crystalline $Na_2O{\cdot}4TeO_2$, which suggests that $Na_2O{\cdot}4TeO_2$ crystallized from all these glasses when heated in DSC.

While the values for T_g or T_m are the same for these glasses, the crystallization temperature varied with the melting temperature, time, or raw material (Fig. 2 and Table II). In general, the crystallization peak moved to lower temperature for the glasses melted at 800°C or for longer time. The effect is more prominent for glasses prepared with $NaNO_3$ (Fig. 2b) compared to that for the glasses prepared with Na_2CO_3 (Fig. 2a).

A comparative analysis for the effect of Na_2CO_3 and $NaNO_3$ on crystallization is shown in Fig. 3 for four different melting conditions, 750°C for 15 min (Fig. 3a), 750°C for 60 min (Fig. 3b), 800°C for 20 min (Fig. 3c) and 800°C for 60 min (Fig. 3d). The crystallization peak for the glass prepared with $NaNO_3$ and melted at 750°C for 15 min (Fig. 3a) is broader and occurs at a higher temperature than the glass prepared under identical melting conditions using Na_2CO_3, which indicates that the glass prepared with $NaNO_3$ is more resistant to crystallization. With longer melting time (60 min) at 750°C, the crystallization peak for the glass prepared with $NaNO_3$ becomes sharper and moves closer to, but still occurs at a higher temperature than, that for the glass prepared with Na_2CO_3, see Fig. 3b and compare with Fig. 3a. Melting at 750°C for 60 min (Fig. 3b) or at 800°C for 20 min (Fig. 3c) the glass prepared with $NaNO_3$ still shows a higher resistance to crystallization than the glass prepared with Na_2CO_3, but not to the extent as when melted at 750°C for 15 min (Fig. 3a). As shown by the identical DSC curves in Fig. 3d, melting at 800°C for 60 min using either $NaNO_3$ or Na_2CO_3 produces identical glasses with respect to their thermal characteristics.

There are several parameters available and used in the literature for describing the stability of glasses against crystallization. These are $\Delta T = T_x - T_g$ [16], $H' = (T_x - T_g)/T_g$ [17, 18], $S = [(T_p - T_x) \cdot (T_x - T_g)]/T_g$ [17, 18], and the Hrüby parameter, $H_r = (T_x - T_g)/(T_m - T_x)$ [19]. The larger ΔT, H', S, or H_r becomes, the larger the stability is for the glass against crystallization. The

TABLE II Characteristic temperatures and various criteria for glass stability against crystallization for the NT_4 glasses

	Melting condition									
Raw materials TeO_2 and	Temp. (°C)	Time (min)	T_g(°C) ±1°C	T_x(°C) ±1°C	T_p(°C) ±1°C	T_m(°C) ±1°C	ΔT(°C) ±1°C	H'	S	Hrüby parameter (hr)
Na_2CO_3	750	15	256	348	364	476	92	0.36	5.75	0.72
	750	60	255	343	357	475	88	0.35	4.83	0.67
	800	20	256	345	359	477	89	0.33	5.00	0.67
	800	60	255	340	355	476	85	0.33	5.00	0.63
$NaNO_3$	750	15	254	367	400	475	113	0.44	14.68	1.05
	750	60	256	350	365	476	94	0.37	5.51	0.75
	800	20	257	357	381	479	100	0.39	9.34	0.82
	800	60	255	340	355	476	85	0.33	5.00	0.63

$H' = (T_x - T_g)/T_g$, $S = (T_p - T_x) \cdot (T_x - T_g)/T_g$, $\Delta T = T_x - T_g$, $H_r = (T_x - T_g)/(T_m - T_x)$.

values for all these parameters for the sodium tellurite glasses, calculated from their DSC curves and given in Table II, also suggest that the glass prepared by melting at 750°C for 15 min and using $NaNO_3$ is the most resistant to crystallization. The stability against crystallization for these glasses decreased in the sequence, $NaNO_3$ (750°C/15 min) > $NaNO_3$ (800°C/20 min) > $NaNO_3$ (750°C/60 min) ≈ Na_2CO_3 (750°C/15 min) > $NaNO_3$ (800°C/60 min) ≈ Na_2CO_3 (750°C/60 min) ≈ Na_2CO_3 (800°C/20 min) ≈ Na_2CO_3 (800°C/60 min).

The above results show that the resistance to crystallization for the glasses prepared with Na_2CO_3 is generally smaller than that for the glasses prepared with $NaNO_3$, although melting at a higher temperature for a longer time, e.g., at 800°C for 60 min, eliminates the difference between the glasses prepared using these two raw materials. It is apparent that melting at 800°C for 60 min produces a common stable melt when either Na_2CO_3 or $NaNO_3$ is used, and this melt stability is reached more quickly when Na_2CO_3 is used, see Fig. 2a. Why a glass prepared by melting at a lower temperature (750°C) for a shorter time (15 min) shows a higher resistance to crystallization when $NaNO_3$ is used is not clearly understood, and, to some degree, surprising.

3.3. Chemical durability and X-ray photoelectron spectra (XPS)

To investigate further why the glass prepared with $NaNO_3$ and melted at a lower temperature for a shorter time (750°C/15 min) had a higher resistance to crystallization, the aqueous chemical durability for these glasses was measured from their dissolution rate (D_R) in water. Also, the surface and interior (∼1.5 nm from the surface obtained by sputtering Ar ions) of the glasses was chemically analyzed by X-ray photoelectron spectroscopy (XPS, Physical Electronics Model 548).

For the measurements of D_R, a clean glass sample, whose dimensions (size) and mass were accurately known, was immersed, using a nylon suspension thread, in de-ionized water (DIW) at room temperature (∼25°C) contained in a plastic bottle. The sample was removed from the bottle after a certain time, washed with DIW and acetone, and dried in air at 90°C for 1 h. The D_R (g/cm^2/min) of the glass was calculated from the difference in its initial and final dimension and weight, and the time it was immersed in water. All measurements were made in duplicate and the average ($\pm 1 \times 10^{-6}$) of these two values is shown in Fig. 4 for four sodium tellurite glasses prepared using $NaNO_3$ or Na_2CO_3 and melted at different temperatures for different times.

Compared to common silicate glasses, the D_R for these sodium tellurite glasses in water is high (poor aqueous chemical durability). However, the DR for the glass prepared with $NaNO_3$ and melted at 750°C for 15 min is a slightly smaller than that for the other glasses, see Fig. 4, which suggests that this glass have a slightly better aqueous chemical durability than the others. A slightly better chemical durability for the ($NaNO_3$/750°C/15min) sodium tellurite glass is consistent with the findings for a higher resistance against crystallization for this glass (Figs 2b or 3a).

It is somewhat surprising to note that the D_R for all these glasses initially increases with increasing time upto 180 min in DIW and then tends to be constant with time >180 min. Generally, D_R for most glasses decreases with time due to the formation of a protective surface layer that retards the rate of dissolution of the glass. It appears no such protective surface layer formed on the surface of these glasses in DIW, at least, in the short time duration (only a few hours) the measurements were conducted.

Fig. 5 compare the N1s XPS spectra on the surface of four representative glasses. The glass melted at 750°C for 15 min using $NaNO_3$ (Fig. 5a) contains a detectable nitrogen (∼5 wt%) on its surface compared to the glasss prepared with Na_2CO_3 (Fig. 5c). The presence of nitrogen on the surface of $NaNO_3$/750°C/15 min glass was confirmed by XPS analysis of a duplicate (glass) sample from the same melt (Fig. 5b). A likely source for this nitrogen is from the decomposition of $NaNO_3$. Since nitrogen has one more bond than oxygen, the presence of nitrogen on the surface of the glass can increase the cross-link density in the glass structure, there by, increasing the chemical durability and resistance to crystallization for the glass. Improving the chemical durability by incorporating nitrogen in the glass has been reported for many oxy-nitride phosphate glasses [20–22]. However, no nitrogen was detected in the interior of this ($NaNO_3$/750°C /15 min) glass, nor was it detected on the surface of the glass prepared with

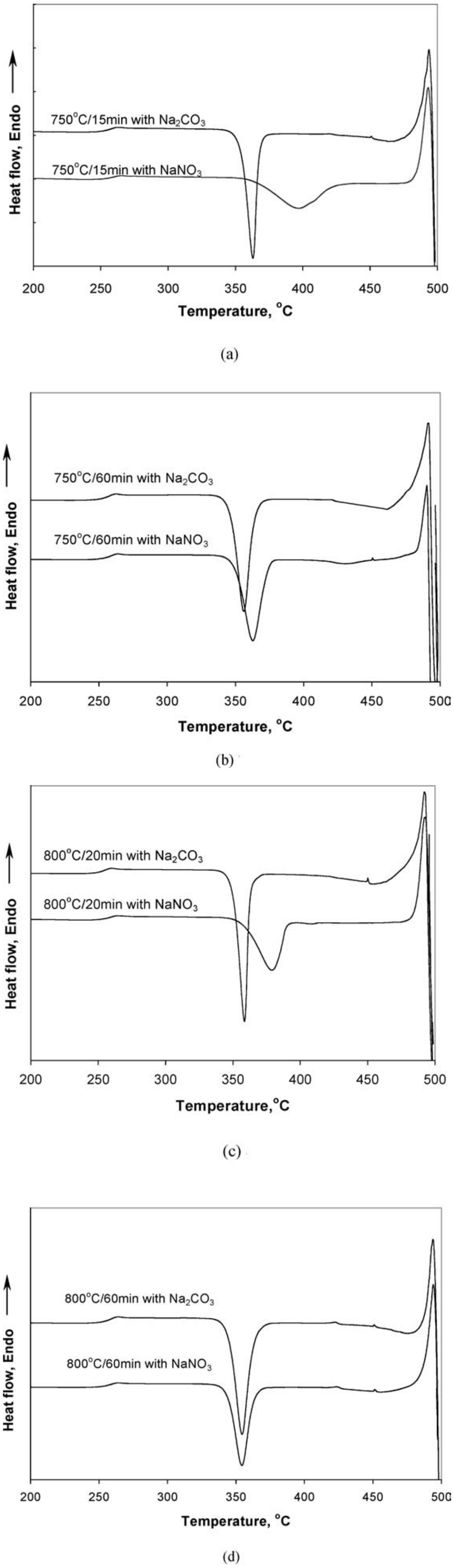

(a)

(b)

(c)

(d)

Figure 3 DSC curves for the NT_4 glass melted at: (a) 750°C for15 min, (b) 750°C for 60 min, (c) 800°C for 20 min, and (d) 800°C for 60 min using Na_2CO_3 or $NaNO_3$.

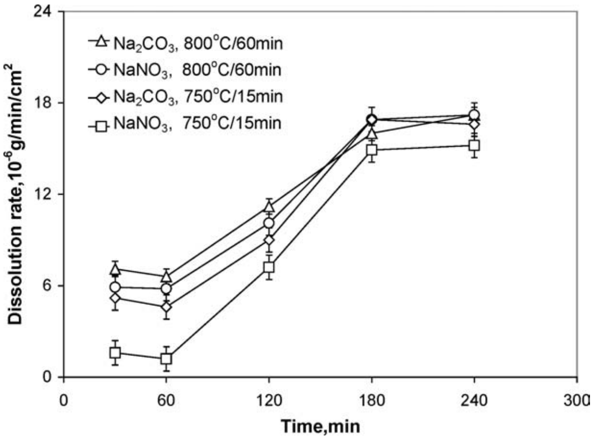

Figure 4 The dissolution rate (D_R) measured in DIW at 25°C for the NT_4 glasses melted at different temperatures for different times using Na_2CO_3 or $NaNO_3$.

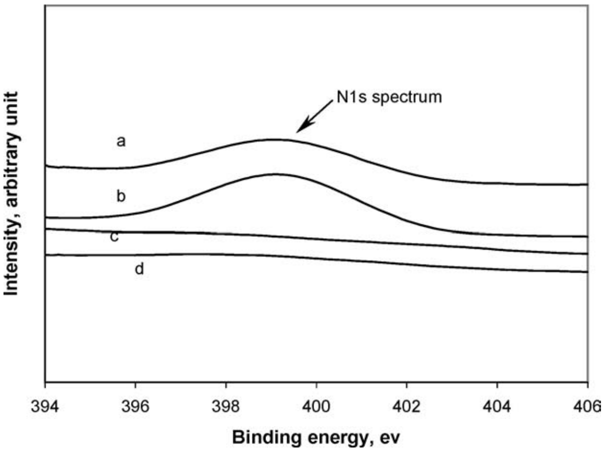

Figure 5 N 1s XPS spectra on the surface of the NT_4 glasses melted at 750–800°C for 15–60 min using $NaNO_3$ or Na_2CO_3: (a) 750°C for 15 min using $NaNO_3$, (b) Duplicate sample from the glass in (a), (c) 750°C for 15 min using Na_2CO_3, and (d) 800°C for 60 min using $NaNO_3$. The curves are intentionally displaced in the vertical direction for clarity.

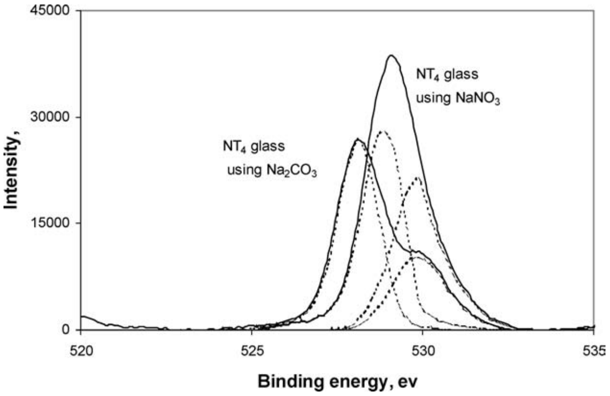

Figure 6 O 1s XPS spectra on the surface for the NT_4 glasses melted at 750°C for 15 min using $NaNO_3$ or Na_2CO_3.

$NaNO_3$, but melted at a higher temperature (800°C) for a longer time (60 min), Fig. 5d. It is believed that melting at a higher temperature for a longer time removed all the nitrogen from the glass melt.

The O 1s XPS spectra in Fig. 6 on the surface of these two glasses, ($NaNO_3$/750°C/15 min) and (Na_2CO_3/750°C/15 min), are also clearly different.

Deconvolution of these spectra indicates that the surface of the glass prepared with $NaNO_3$ contains a smaller number of non-bridging oxygen (NBO, ~30%) than that of the glass prepared with Na_2CO_3 (NBO, ~50%). A smaller fraction of NBO on the glass surface can also contribute to the higher chemical durability or higher resistance to crystallization for this ($NaNO_3$/750°C/15 min) glass. In the alkali tellurite glasses [23], NBO forms as the TeO_4 trigonal bi-pyramids (tbp's) are converted to TeO_3 trigonal pyramids (tp's). Thus, it is suspected that the ($NaNO_3$/750°C/15 min) glass contains a higher fraction of TeO_4 tbp's on its surface than the (Na_2CO_3/750°C/15min) glass. As was observed for the N 1s spectra, the O 1s spectra in the interior of both glasses are also the same.

3.4. IR spectra

The IR spectra for the glasses prepared using Na_2CO_3 and $NaNO_3$ are shown in Fig. 7a and b, respectively, as a function of melting temperature and time. Since all the important absorptions for the alkali tellurite glasses are between 400–1000 cm^{-1}, only that part of the IR spectra is shown in Fig. 7. No significant difference in the IR spectra for these glasses is observed with changing melting temperature, time, or raw material. The general features of these spectra are typical of alkali-tellurite glasses [9, 24], which contain only a broad absorption band between 590 and 810 cm^{-1}. The most pronounced absorption near 600 cm^{-1} is attributed to the asymmetric stretching vibrations of $Te–O_{ax}$ bonds, and that near 800 cm^{-1} is attributed to the symmetric stretching vibrations of $Te–O_{eq}$ bonds [9, 24–26] in the deformed TeO_4 (tbp) units. It has been suggested [25, 27] that part of the absorption near 800 cm^{-1} is also caused by the symmetric stretching vibrations of Te–O bonds in the TeO_3 pyramidal units.

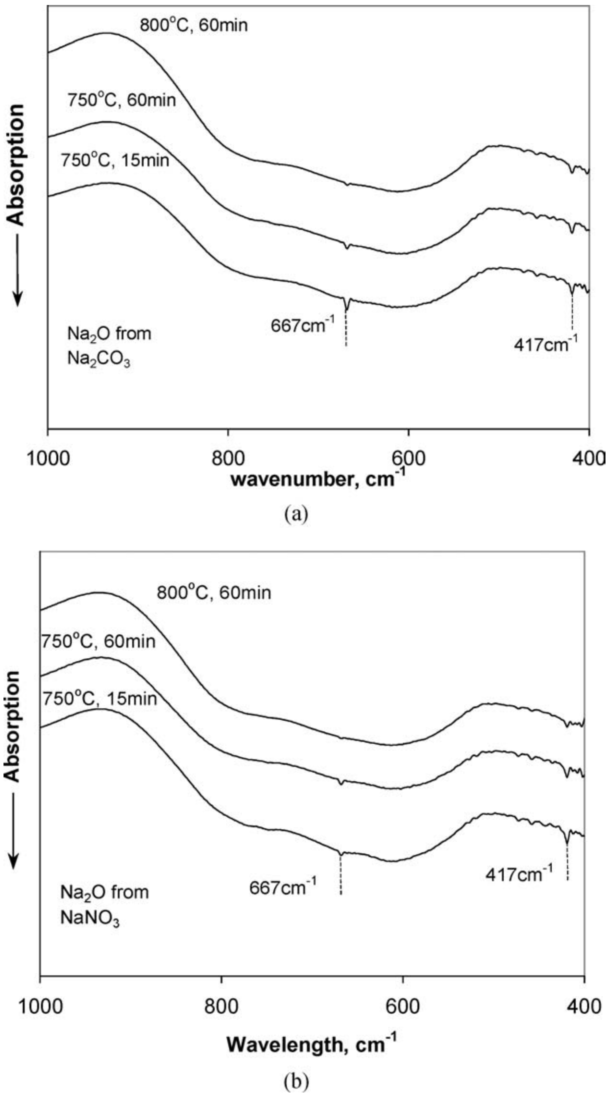

Figure 7 IR spectra for the NT_4 glasses melted at different temperatures for different times using: (a) Na_2CO_3 or (b) $NaNO_3$.

The close similarity of the IR spectra in Fig. 7 indicates that there is basically no difference in the structure of these glasses, irrespective of their melting temperature, time, or starting raw material, which is expected. However, a closer inspection show that the absorption near 600 cm^{-1} for the glass made with $NaNO_3$ and melted at 750°C for 15 min is a little larger, see Fig. 7b, compared to that for the other glasses. Although small, this difference (in the IR spectra) may be considered real, if the observed difference in the DSC pattern for this ($NaNO_3$/750°C/15 min) glass, compared to the DSC patterns for other glasses (Fig. 2b), is taken into account. A deeper absorption near 600 cm^{-1} may indicate that the concentration of $Te—O_{ax}$ bonds in this glass is a little higher than that in the other glasses. However, how a higher concentration of the $Te—O_{ax}$ bonds is related to a higher resistant to crystallization (DSC in Fig. 2b) is not understood.

Also, a few small, but sharp absorption peaks (~667 cm^{-1}, and near 417 cm^{-1}) are observed in the IR spectra for these glasses, which maybe some kind of experimental artifacts. However, the peak at ~667 cm^{-1} disappears when the glass is melted at higher temperatures for longer times, e.g., at 800°C for 60 min, suggesting a structural change in the glass network Measurements on duplicate samples reproduced the same results, i.e., presence of the peak in glasses melted at lower temperature for shorter times and absence of the peak in glasses melted at higher temperature for longer times. The origin of this peak, which cannot be correlated with any of the absorption peaks for water, remains unknown at this time. It may be worth mentioning that a similar small absorption (~667 cm^{-1}) was also present in the IR spectra reported by Heo *et al.* [9] for sodium tellurite glasses, although they did not mention or discuss for the origin of this absorption. The IR spectra reported by the same authors [9] for the lithium tellurite glasses did not contain any such absorption, so the absorption at ~667 cm^{-1} for the sodium tellurite glasses cannot be related, at least, to any kind of Te–O vibrations.

3.5. XRD analysis of samples

The glasses melted at 800°C for 60 min using Na_2CO_3 or $NaNO_3$ were crystallized at 350°C for 10 h, and then analyzed by XRD, see Fig. 8. The XRD pattern for crystalline $Na_2O \cdot 4TeO_2$ (NT_4) is also included in Fig. 8 for comparison. As shown in Fig. 8, the XRD

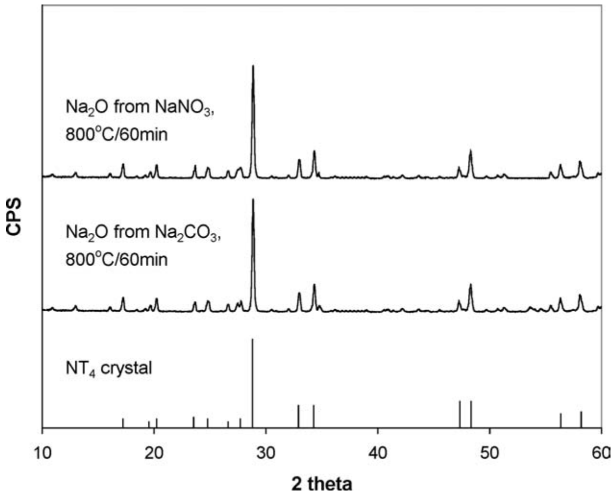

Figure 8 XRD spectra for the NT$_4$ glasses after crystallizing at 350°C for 10 h. The temperature and time for melting and the raw materials used to prepare the glasses are shown on the respective plots.

peaks for the crystallized samples match well with those for crystalline NT$_4$ [27]. These sodium tellurite glasses always crystallized only NT$_4$ crystals when heat-treated regardless of the raw material used for Na$_2$O.

4. Conclusions

The crystallization tendency of the sodium tellurite glasses is influenced by the melting temperature and time, and also by the type of raw material (NaNO$_3$ or Na$_2$CO$_3$) used as a source for Na$_2$O to prepare these glasses. Melting at 750°C for 15 min and using NaNO$_3$ produced a glass that is slightly more chemically durable and more resistant to crystallization than glasses prepared by melting for longer time (60 min at 750°C), or at a higher temperature (800°C), or using Na$_2$CO$_3$ as a source for Na$_2$O. The glass prepared using NaNO$_3$ and melted at 750°C for 15 min is believed to have a thin nitrogen rich surface layer ($<$1.5 nm) and a higher proportion of BO, which is suspected to be the reason for its higher chemical durability and higher resistance to crystallization than the other sodium tellurite glasses investigated in this work. However, this glass appears to be less stable, since the apparently improved properties, namely, the chemical durability and resistant to crystallization, are found to change with melting temperature and time. Melting at a slightly higher temperature, 800°C, or for a longer time (60 min) at 750°C produces a more stable glass, whose properties remain invariant with the type of raw material, NaNO$_3$ or Na$_2$CO$_3$, used for the source of Na$_2$O.

Acknowledgment

This work is supported by the National Aeronautics and Space Administration (NASA), Grant NAG8-1465.

References

1. J. E. STANWORTH, *J. Soc. Glass Technol.* **36** (1952) 217.
2. H. BURGER, W. VOGEL and V. KOZHUKHAROV, *Infrared Phys.* **25** (1985) 395.
3. H. NASU, O. MATSUSHITA, K. KAMIYA, H. KOBAYASHI and K. KUBODERA, *J. Non-Cryst. Solides* **124** (1990) 275.
4. S. H. KIM, T. YOKO and S. SAKKA, *J. Amer. Ceram. Soc.* **76** (1993) 865.
5. *Idem. ibid.* **76** (1993) 2486.
6. A. A. BAHGAT, E. E. SHAISHA and A. I. SABRY, *J. Mater. Sci.* **22** (1987) 1323.
7. C. S. RAY, D. E. DAY, M. MAKIHARA and J. HAYAKAWA, in "19th ISTS," edited by M. Hinada (Hakushinsha Co., Tokyo, Japan, 1994) p. 651.
8. D. ZHU, W. ZHOU and C. S. RAY, *J. Mater. Sci. Lett.* **20** (2001) 1961.
9. J. HEO, D. LAM, G. H. SIGEL, E. A. MENDOZA and D. A. HENSLEY, *J. Amer. Ceram. Soc.* **75** (1992) 77.
10. S. K. LEE, M. TATSUMISAGO and T. MINAMI, *Phys. Chem. Glass.* **35** (1994) 226.
11. A. MOGUŠ-MILANKOVIĆ, A. ŠANTIĆ, K. FURIĆ, C. S. RAY and D. E. DAY, *J. Eur. Ceram. Soc.* (in press).
12. T. SEKIYA, N. MOCHIDA, A. OHTSUKA and M. TANOKAWA, *J. Non-Cryst. Solids* **144** (1992) 128.
13. S. L. TAGG, R. E. YOUNGMAN and J. W. ZWANZIGER, *J. Phys. Chem.* **99** (1995) 5111.
14. N. KITAMURA, M. MAKIHARA, T. SATO, M. HAMAI, I. MOGE, S. AWAJI, K. WATANABE and M. MOTOKAWA, *JASMA* **17** (2000) 102.
15. B. P. TROITSKII, A. K. YAKHKIND and N. S. MARTYSHCHENKO, *Izv. Akad. Nauk SSSR, Neorg. Mater.* **3** (1967) 741.
16. A. DIETZEL, *Glastechn. Ber.* **22** (1948/1949) 41.
17. Y. MESSADDEQ and M. POULAIN, *J. Non-Cryst. Solids* **140** (1992) 41.
18. N. P. BANSAL, A. J. BRUCE, R. H. DOREMUS and C. T. MOYNIHAN, *ibid.* **70** (1985) 379.
19. A. HRÜBY, *J. Phys.* B **22** (1972) 1187.
20. D. E. DAY and M. R. REIDMEYER, *J. Non-Cryst. Solids* **181** (1995) 201.
21. D. E. DAY, *ibid.* **112** (1989) 7.
22. D. E. DAY, M. R. REIDMEYER and R. K. BROW, *ibid.* **177** (1994) 208.
23. Y. HIMEI, Y. MIURA, T. NANBA and A. OSAKA, *ibid.* **211** (1997) 64.
24. T. YOKO, K. KAMIYA, H. YAMADA and K. TANAKA, *J. Amer. Ceram. Soc.* **71** (1988) C70.
25. Y. DIMITRIEV, V. DIMITROV and M. ARNAUDOV, *J. Mater. Sci.* **18** (1983) 1353.
26. T. UCHINO and T. YOKO, *J. Non-Cryst. Solids* **204** (1996) 243.
27. R. A. EL-MALLAWANY, *Infrared Phys.* **29** (1989) 781.
28. International Center For Diffraction Data, PCPDFWIN Version 2.01, 1998.

Received 16 July 2003
and accepted 3 June 2004